PHYSICAL REVIEW E VOLUME 53, NUMBER 1 JANUARY 1996

Topological interactions in model polymer networks

Ralf Everaers* and Kurt Kremer†
Theorie II, Institut für Festkörperforschung, Forschungszentrum Jülich, Postfach 1913, D-52425 Jülich, Germany
(Received 3 March 1995)

We numerically analyze mesh entanglements in model polymer networks. We find $G-G_{ph}\approx 0.85\rho_{ent}k_BT$, where ρ_{ent} is the entanglement density, G the shear modulus which was measured in extensive molecular dynamics simulations of stretched samples, and G_{ph} the phantom model prediction for the equivalent system without topological constraints. A simple model calculation of the prefactor is in close agreement with the observed value.

PACS number(s): 61.41.+e, 02.40.Pc, 05.90.+m

Rubberlike materials have unique elastic properties [1]. Qualitatively, they have been understood for 60 years following the realization that a flexible, randomly coiled polymer in a melt can be viewed as a linear entropic spring [2]. The statistical mechanics of polymer networks is, however, a complicated and still unsolved problem. Similarly to spin glasses [3] they contain quenched disorder, a point first fully appreciated by Edwards [4,5]. Particularly difficult to handle are the topological constraints due to the mutual impenetrability of the chains. Their mere specification requires an — in principle infinite — set of topological invariants for pairs, triples, etc. of loops [5]. In contrast to computer simulations [6] experiments can neither test nor provide microscopic input for topological theories of rubber elasticity. Purely analytic attempts are very complex [7–9] and have not led to a satisfactory conclusion. Alternative approaches try to approximate the global *topological* constraints by local *geometrical* constraints on strands [10–15]. The tube model [10–12], in particular, is very successful and provides a unified view on networks and entangled polymer melts on a mean-field level. Simulations [16–18] as well as experiments [19,20] back up the microscopic picture of a tube. It is an open question whether these simpler models can be derived from more fundamental topological considerations [21].

In this paper we use computer simulations to explore the original ansatz of Edwards [4,5] to consider only one type of "entanglement:" linked loops. Most topological theories of rubber elasticity [7–9,13] are based on this idea. In a previous paper [22] we have introduced randomly interpenetrating polymer networks with diamond lattice connectivity as a convenient starting point for a systematic study of quenched topological disorder in rubberlike materials. These systems were investigated under elongational strain allowing us to determine shear moduli G from the restoring forces. Here we calculate the degree of linking for all mesh pairs in our systems. This microscopic information allows us to directly test the model of Graessley and Pearson [13] (GP), because it predicts the topology contribution to the shear modulus on the basis of a well-defined microscopic picture for the interaction between entangled loops. This makes the GP theory particularly suited for testing the foundations of topological theories of rubber elasticity in a computer simulation.

The link contribution to the shear modulus. The reference system for the assessment of the consequences of topology conservation is the "phantom" network [23,24], where the chains may pass freely through their neighbors and themselves. The model forms the basis of most modern theories of rubber elasticity [11,12,25–27]. Note that in dense systems it is topology conservation and *not* the screened excluded volume interaction that causes deviations from the phantom network behavior [28,29]. To motivate a contribution of links to the modulus we follow an idea of Vologodskii *et al.* (VK) [30]. They defined an entropic interaction between loop centers of mass (c.m.) due to the *conservation* of the topological state of a loop pair. Consider two rings of length N with a c.m. distance $\vec{r}$. There is a certain probability $f_N(\vec{r})$ for them to be linked. In the following, we will assume the existence of a suitably defined characteristic distance of entangled meshes, the linking radius $R_L(N)$, which can be used to scale the linking probabilities, i.e., $f_N(\vec{r})=f(\vec{r}/R_L(N))$. The change in entropy due to a modification $\overleftrightarrow{\lambda}$ of the distance is $k_B\{\ln[f(\overleftrightarrow{\lambda}\vec{x})]-\ln[f(\vec{x})]\}$, if they are linked, and $k_B\{\ln[1-f(\overleftrightarrow{\lambda}\vec{x})]-\ln[1-f(\vec{x})]\}$, if they are not linked. Unfortunately, the linking probability $f(\vec{x})$ and its dependence on the size of the loops are not generally known [30–32].

Applying these ideas to polymer networks GP assumed [13] (i) that the loops are randomly distributed in space with a density ρ_{loop}, (ii) that the contributions of the different loop pairs are independent and additive, (iii) that the linking probability $f(\vec{x})$ depends only on the distance $|\vec{x}|$ and not on the distortion of the loop shapes in the course of the deformation, and (iv) that the positions of the loop c.m. change affinely with the deformation $\overleftrightarrow{\lambda}$ of the sample. The GP result for the contribution G_{ent} to the shear modulus can be written as

$$G_{ent}=\mathscr{A}[f(x)]\rho_{ent}k_BT, \tag{1}$$

*Present address: Institut Charles Sadron, 6, rue Boussingault, F-67083 Strasbourg CEDEX, France.

†Permanent address: Max-Planck Institut für Polymerforschung, Postfach 3148, D-55021 Mainz, Germany.

TABLE I. Strand length N, total number of particles N_{mon}, true shear modulus G, phantom model shear modulus G_{ph} for the equivalent system without topological constraints and the estimate G_{ent} of the Graessley and Pearson model for the loop entanglement contribution.

N	N_{mon}	G $[\epsilon/\sigma^3]$	G_{ph} $[\epsilon/\sigma^3]$	G_{ent} $[\epsilon/\sigma^3]$
12	8000	0.100 ± 0.003	0.072	0.042
26	23744	0.060 ± 0.003	0.035	0.036
44	51264	0.041 ± 0.002	0.020	0.032

$$\rho_{ent}=2\pi\rho_{loop}^2R_L^3\int_0^\infty x^2f(x)dx, \tag{2}$$

$$\mathscr{A}[f(x)]=\frac{1}{15}\frac{\int_0^\infty \frac{x^4f'^2(x)}{f(x)[1-f(x)]}dx}{\int_0^\infty x^2f(x)dx}. \tag{3}$$

Assuming further that (v) up to a prefactor a_0 of order 1 the effect of topology conservation can be identified with G_{ent} and (vi) that this contribution is independent of and additive to the modulus G_{ph} of the phantom network without topological constraints the total shear modulus G is given by

$$G=G_{ph}+a_0\mathscr{A}[f(x)]\rho_{ent}k_BT. \tag{4}$$

Note that Eqs. (1)–(4) implicitly assume that simple link topologies dominate and that it is not necessary to distinguish between different types of entanglement.

The simulation model. For our simulations [22] we used the same coarse-grained model as in earlier investigations of polymer melts and networks [16,18]. The network strands were modeled as freely jointed bead spring chains of uniform length N. There were two types of interactions, an excluded volume interaction, U_{LJ}, between all monomers and a bond potential, U_{FENE}, between chemical nearest neighbors. With ϵ, σ, and τ as the Lennard-Jones units of energy, length, and time we worked at a temperature $k_BT=1\epsilon$ and at a density $\rho=0.85\sigma^{-3}$. The average bond length was $l=0.97\sigma$ and topology was conserved. The relevant length and time scales for chains in a melt are the mean-square end-to-end distance $\langle R^2\rangle(N)\approx1.7l^2N$, the melt entanglement length $N_e\approx35$ monomers, and the Rouse time $\tau_{Rouse}\approx1.5N^2\tau$ [16]. We carried out molecular dynamics simulations, where the system was weakly coupled to a heat bath. Simulation times were of the order of $10\tau_{Rouse}$, while the stress relaxation in strained samples was completed after about $2\tau_{Rouse}$. The short relaxation times are due to the defect-free structure of our networks.

The strands were cross-linked by four-functional monomers into networks with the connectivity of a diamond lattice and placed in a commensurable, cubic simulation box with periodic boundary conditions. The bond length of the diamond lattice (identical to the mean elongation of the strands) was set to $\langle R^2(N+1)\rangle^{1/2}$ of the melt chains. The diamond networks were prepared and relaxed as phantom networks with the correct melt persistence length [18]. To reach melt density we superimpose $n\sim N^{1/2}$ diamond networks in the simulation volume which interpenetrate each other randomly. By introducing the excluded volume interaction between all monomers the topology is quenched and as in realistic systems there are of the order of $N^{1/2}$ cross-links in the volume of one chain. The density of elastically active strands is given by $\rho_{strand}=\rho/(N+1/2)$. We have investigated systems with strand lengths $N=12,26,44$ (Table I) corresponding to $n=5,7,9$ independent, but mutually interpenetrating diamond networks. The total number of particles ranged from 8000 and to 51 264 monomers. A phantom network with these characteristics has a modulus of $G_{ph}=\rho_{strand}k_BT$ [22]. The true shear moduli, which we obtained from the restoring forces in simulations of strained samples, are significantly higher (Table I) but nevertheless of *purely entropic origin*. For more details we refer to Ref. [22].

TABLE II. Linking statistics for meshes in randomly interpenetrating polymer networks with diamond lattice connectivity. Listed are the number of loops N_{loop}, the total number of linked pairs of loops N_{link}, the number of links with a GLN larger than one $N_{link}^{|I|>1}$, the number of links between meshes on identical diamond networks N_{link}^{intra}, the radius of gyration of the meshes R_g and the linking radius R_L.

N	N_{loop}	N_{link}	$N_{link}^{\lvert I\rvert>1}$	N_{link}^{intra}	R_g	R_L
12	640	11120	124	32	4.57 ± 0.03	4.22 ± 0.03
26	896	28508	1478	146	6.74 ± 0.04	6.50 ± 0.03
44	1152	54701	4511	254	8.79 ± 0.06	8.69 ± 0.04

Analysis of link topologies. We use the Gauss linking number (GLN)

$$I=\frac{1}{4\pi}\oint\oint\frac{(d\vec{r}_1\times d\vec{r}_2)\cdot(\vec{r}_1-\vec{r}_2)}{|\vec{r}_1-\vec{r}_2|^3}=0,\pm1,\ldots \tag{5}$$

to distinguish between entangled ($I\neq0$) and nonentangled pairs of loops or meshes. Similarly to Eqs. (1)–(4) the use of the GLN is only justified for simple link topologies [5,30,33]. Note that in contrast to algebraic invariants the GLN can be integrated into the standard polymer formalism [7,33]

Iwata [8] pointed out that it is sufficient to consider only the meshes of a network, since for any larger loop the Gauss integral can be written as a sum over GLNs for mesh pairs. The diamond lattice cannot be partitioned into a set of its meshes which consist of six strands and cross-links. We therefore consider all $N_{loop}=N_{strand}$ different meshes, but set $\rho_{loop}=\frac{1}{6}N_{loop}/V$ and $\rho_{ent}=\frac{1}{36}N_{link}/V$ [29]. The direct evaluation of the GLN [Eq. (5)] for a pair of loops is an order $[6(N+1)]^2$ operation and quite time-consuming. Instead we first apply a simple smoothing operation to the rings [34].

The result of evaluating Eq. (5) for all pairs of elementary meshes is listed in Table II. At most 10% of the links in our systems have a GLN of 2 or more, i.e., the simple link topologies, for which the derivation of Eqs. (1)–(4) and the use of the GLN is justified, do in fact dominate. For the subsequent determination of the linking probabilities we neglect

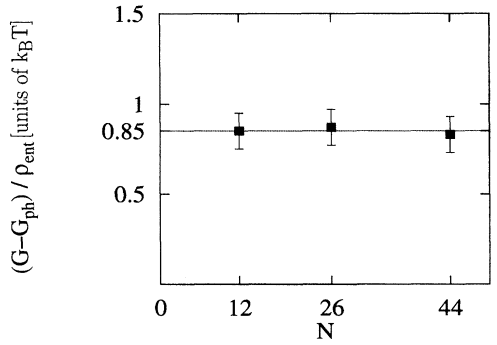

FIG. 1. Strand length dependence of the ratio of the topology contribution $G-G_{ph}$ to the shear modulus and the entanglement density ρ_{ent}.

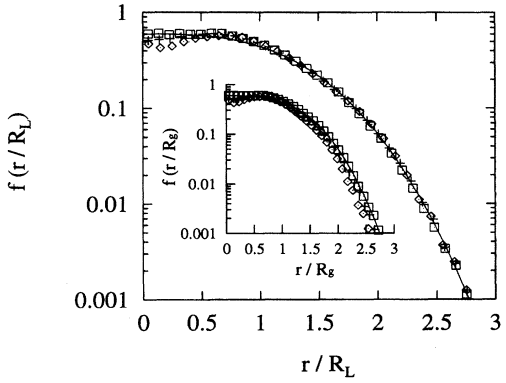

FIG. 2. Scaling of the linking probability $f(r)$ for meshes in randomly interpenetrating polymer networks with diamond lattice connectivity with the linking radius R_L: $N=44$ (□), $N=26$ (+), ($N=12$) (◇). The solid line shows the approximate form Eq. (7). The inset demonstrates that the data do not scale as well with the mesh radius of gyration R_g.

pairs of distant neighbor meshes on identical diamond networks, which account for less than 0.5% of the total number of links. We therefore do not have to worry about correlations in the loop positions or about the effective reduction of the loop density due to the fact that the GLN is not defined for pairs of loops with common points.

Entanglement density and shear modulus. Step one in our analysis is to confirm the proportionality of the loop entanglement density ρ_{ent} and the *total* topology contribution $G-G_{ph}$ to the modulus Eq. (4). Figure 1 illustrates our key result:

$$\frac{G-G_{ph}}{\rho_{ent}}=0.85k_BT, \tag{6}$$

independent of chain length and although each loop has overlap with of the order of $n=5,7,9>3$ other loops. This observation suggests that — at least in the present case — pair interactions dominate over higher order terms. Step two is a consistency test based on the GP estimate Eq. (3) of the prefactor.

Figure 2 shows the linking probabilities for different chain lengths calculated from pair correlation functions for the c.m. of (linked) loops. The data are well described by the functional form

$$f_N(\vec{r})\approx\alpha\,\exp\left(-\frac{\alpha}{2}\frac{r^3}{R_L^3}\right), \tag{7}$$

with $\alpha=0.6$. This ansatz follows from a similar form proposed by VK [30], if we define $(4\pi/3)R_L^3=\frac{1}{2}\int d^3r f_N(\vec{r})$. The linking radii R_L can be determined from the data in Table II [35]. Using Eq. (7) we can calculate the absolute, *parameter-free* prediction of the GP ansatz [Eqs. (1) and (3)]

$$\frac{G_{ent}}{\rho_{ent}}=\mathscr{A}[f(x)]k_BT=1.3k_BT, \tag{8}$$

which is in excellent agreement with Eq. (6). Thus, we not only observe the predicted proportionality of ρ_{ent} and $G-G_{ph}$, but the GP theory also provides an estimate of the prefactor that agrees with the measured value up to a numerical constant $a_0=(G-G_{ph})/G_{ent}\approx 2/3$ of order 1.

As a last point we address the strand length dependence of ρ_{ent}. We note that ρ_{ent} exceeds the value $(n-1)\rho_{loop}$ for regular interpenetration by a factor between 1.4 ($N=12$) and 2.0 ($N=44$). Consequently, for the chain lengths considered R_L grows marginally faster than the mesh radius of gyration R_g (Table II, see also the inset in Fig. 2). A similar finite-size effect was observed by VK [30] and is also detectable in the data of Iwata [32]. Note that the simple entanglement definition we used in this paper has to break down for large N: $G_{ent}\sim\rho_{ent}\sim\rho_{loop}^2R_L^3\sim N^{-0.5}$ vanishes and cannot explain an asymptotic shear modulus of the order of the melt plateau modulus. Future work has to address more complicated two loop interactions as well as multiloop entanglements.

Summary and conclusion. The present work is a *quantitative* implementation of a topological theory of rubber elasticity. Considering the crudeness of the model its success is remarkable and should motivate further work along these lines. We have performed an analysis of loop entanglements in model polymer networks which were investigated by molecular dynamics simulations [22]. We found that in these systems the difference between the actual modulus G and the phantom network modulus G_{ph} is proportional to the density ρ_{ent} of entangled mesh pairs. The result confirms ideas of Edwards [4,5], Vologodskii *et al.* [30], and Graessley and Pearson [13] which allow one to estimate the proportionality factor up to a constant of order 1.

Discussions with G. S. Grest are gratefully acknowledged. This work was supported by a generous CPU time grant from the German Supercomputer Center HLRZ (Jülich) within the Disordered Polymer Project and by a NATO travel grant (No. 86680). R.E. acknowledges partial support from SFB262 of the Deutsche Forschungsgemeinschaft DFG.

[1] L. R. G. Treloar, *The Physics of Rubber Elasticity* (Clarendon, Oxford, 1975).

[2] E. Guth and H. Mark, Monats. f. Chemie **65**, 93 (1934); W. Kuhn, Kolloid Zeits. **76**, 258 (1936).

[3] M. Mezard, G. Parisi and M. V. Virasaro, *Spinglass Theory and Beyond* (World Scientific, Singapore, 1987).

[4] S. F. Edwards, Proc. Phys. Soc. **91**, 513 (1967).

[5] S. F. Edwards, J. Phys. A **1**, 15 (1968).

[6] R. Everaers, K. Kremer, and G. S. Grest, Macromol. Symposia **93**, 53, (1995).

[7] R. T. Deam and S. F. Edwards, Philos. Trans. R. Soc. London Ser. A **280**, 317 (1976).

[8] K. Iwata, J. Chem. Phys. **76**, 6363 (1982).

[9] K. Iwata, J. Chem. Phys. **83**, 1969 (1985).

[10] M. Doi and S. F. Edwards, *The Theory of Polymer Dynamics* (Clarendon Press, Oxford, 1986).

[11] S. F. Edwards and T. A. Vilgis, Rep. Prog. Phys. **51**, 243 (1988).

[12] G. Heinrich, E. Straube, and G. Helmis, Adv. Pol. Sci. **85**, 34 (1988).

[13] W. W. Graessley and D. S. Pearson, J. Chem. Phys. **66**, 3363 (1977).

[14] R. C. Ball, M. Doi, S. F. Edwards, and M. Warner, Polymer **22**, 1010 (1981).

[15] P. G. Higgs and R. C. Ball, Europhys. Lett. **8**, 357 (1989).

[16] K. Kremer and G. S. Grest, J. Chem. Phys. **92**, 5057 (1990); **94**, 4103 (1991) (Erratum).

[17] W. Paul, K. Binder, D. W. Heermann and K. Kremer, J. Chem. Phys. **95**, 7726 (1991).

[18] E. R. Duering, K. Kremer, and G. S. Grest, J. Chem. Phys. **101**, 8169 (1994).

[19] D. Richter, L. Willner, A. Zirkel, B. Farago, L.J. Fetters, and J. S. Huang, Phys. Rev. Lett. **71**, 4158 (1993).

[20] E. Straube, V. Urban, W. Pyckhout-Hintzen, D. Richter, and C. J. Glinka, Phys. Rev. Lett. **74**, 4464 (1995).

[21] K. Iwata and S. F. Edwards, J. Chem. Phys. **90**, 4567 (1989).

[22] R. Everaers and K. Kremer, Macromolecules **28**, 7291 (1995).

[23] H. James and E. Guth, J. Chem. Phys. **11**, 455 (1943).

[24] P. J. Flory, Proc. R. Soc. London Ser. A **351**, 351 (1976).

[25] B. Erman and P. J. Flory, Macromolecules **15**, 800 (1982).

[26] P. G. Higgs and R. C. Ball, J. Phys. (Paris) **49**, 1785 (1988).

[27] P. M. Goldbart and A. Zippelius, Phys. Rev. Lett. **71**, 2256 (1993).

[28] R. C. Ball and S. F. Edwards, Macromolecules **13**, 748 (1980).

[29] R. Everaers, Ph.D. thesis, University of Bonn, 1994, published in Berichte des Forschungszentrums Jülich, Jül-3040 (1995); R. Everaers and K. Kremer (unpublished).

[30] A. V. Vologodskii, A. V. Lukashin and M. D. Frank-Kamenetskii, Zh. Eksp. Teor. Fiz. **67**, 1875 (1974) [Sov. Phys. JETP **40**, 932 (1975)]; M. D. Frank-Kamenetskii, A. V. Lukashin and A. V. Vologodskii, Nature **258**, 398 (1975).

[31] K. Iwata and T. Kimura, J. Chem. Phys. **74**, 2039 (1981).

[32] K. Iwata, J. Chem. Phys. **78**, 2778 (1983).

[33] F. W. Wiegel, *Introduction to Path Integral Methods in Physics and Polymer Science* (World Scientific, Philadelphia, 1986).

[34] K. Koniaris and M. Muthukumar, Phys. Rev. Lett. **66**, 2211 (1991).

[35] $$R_L=\left(\frac{3}{4\pi}\frac{N_{mon}}{\rho}\frac{n}{n-1}\frac{N_{link}-N_{link}^{intra}}{N_{loop}^2}\right)^{1/3}.$$